Electrochemical Materials and Technologies

ARTICLE

eISSN: 2949-0561

Cite this: Electrochem. Mater. Technol. 5 (2026) 20265065

High-temperature processing of nitride spent fuel. Theoretical foundations. Part I

Alexei Potapov [a]*, Mikhail Mazannikov [a], Yuriy Zaikov [a]

Received: 19 November 2025
Accepted: 20 January 2026
Published online: 4 February 2026

DOI: 10.15826/elmattech.2026.5.065

High-temperature processing (HTP) of nitride spent nuclear fuel (SNF) is a series of head-end operations, as a result of which the fuel cladding is removed and the main components of the fuel (uranium and plutonium) are converted into pressable UO_2 and PuO_2 oxides. Based on the properties of uranium nitrides and oxides, a high-temperature processing (HTP) scheme for nitride spent nuclear fuel is proposed. This scheme consists of nitriding, denitriding, cladding separation, uranium oxidation to U_3O_8, and subsequent reduction to UO_2. Theoretical and thermodynamic justification for each HTP stage is provided.

keywords: pyrochemical processing, spent nuclear fuel, uranium nitride, uranium oxide, nitriding, voloxidation

1. Introduction

High-temperature processing (HTP) of nitride spent nuclear fuel (SNF) is a series of key technological operations in the pyrochemical scheme of SNF reprocessing. Their goals are to extract fuel from the fuel element cladding, separate volatile fission products and convert nitrides into oxides (UO_2, PuO_2, ZrO_2, La_2O_3, CeO_2, Nd_2O_3, etc.), which will be used in the next stage of processing – electrochemical reduction to metals [1–3]. This approach implies a development of the scheme described in [4]. HTP can be used for both nitride and oxide fuels. The oxidation of oxide fuel by air or other oxygen-containing gas mixtures has been previously studied and described in many works, for example [5–8]. In successive transformations, oxides with one crystal lattice are transformed into oxides with another lattice, Table 1.

This promotes fuel grinding and the release of volatile fission products. In addition, according to the data reported in Table 1, in row (5) there is an increase in the volume of fuel, which can cause the destruction of the cladding, which significantly facilitates the separation of the cladding and fuel.

The main interaction reaction between uranium dioxide and oxygen is as follows (1):

$$UO_2 + 0.333O_2 = 0.333U_3O_8,\quad \Delta G = -68.2\ \text{kJ at } 500\ °\text{C} \tag{1}$$

Below 500 °C, deeper oxidation reactions can occur (2), (3):

$$U_3O_8 + 0.5O_2 = 3UO_3,\quad t < 500\ °\text{C},\ \Delta G = -19\ \text{kJ at } 500\ °\text{C} \tag{2}$$

$$U_3O_8 + 0.333O_3 = 3UO_3,\quad t < 200\ °\text{C},\ \Delta G = -109\ \text{kJ at } 200\ °\text{C} \tag{3}$$

Other gases have also been studied, for example, nitrogen (IV) oxide [11, 12]. In this case, the following Reactions (4), (5) occur:

a: Institute of High-Temperature Electrochemistry Ural Branch, Russian Academy of Sciences, Ekaterinburg 620066, Russia

* Corresponding author: a.potapov_50@mail.ru

$$UO_2 + 0.667NO_2 = 0.333U_3O_8 + 0.667NO, \quad t \geq 350\ °C, \Delta G = -68\ kJ \text{ at } 350\ °C \tag{4}$$

$$U_3O_8 + NO_2 = 3UO_3 + NO, \quad 150\ °C \leq t < 350\ °C, \Delta G = -24\ kJ \text{ at } 350\ °C \tag{5}$$

Oxygen and various Ar + O_2 mixtures can also be used to oxidize nitride spent nuclear fuel. Oxidation occurs rapidly and generates significant heat (see Section 2.4.1.). However, the use of air and other oxygen-containing mixtures has a number of disadvantages, such as possible oxidation of the cladding and possible contamination of the fuel with oxidation products. The second disadvantage is the conversion of some volatile components into low-volatile oxides, primarily cesium and rubidium (Cs_2UO_4, Rb_2UO_4).

In this paper, treatment with nitrogen is proposed at the first stage of HTT. Nitrogen does not interact with structural materials (EP 823 steel), does not prevent the release of volatile fission products, and allows the release of the cladding due to an increase in the volume of fuel during the UN oxidation to (U_2N_3 + UN_2) mixture.

The main elements that compose nitride SNF are uranium, followed by plutonium and fission products. The composition of SNF varies depending on the initial plutonium content, the burn-up, and the holding period in the off-reactor storage facility.

In this paper, for the sake of certainty, we will have in mind the model fuel, the composition of which is given in Table 2. This table is compiled according to the data reported in [13–15]. The ratio is UN–PuN ≈ 0.84–0.16, and the sum UN + PuN ≈ 91.6 mol. %.

Only uranium nitride participates in reactions with nitrogen. Neither plutonium nitride nor the majority of fission products interact with nitrogen. Therefore, the stages of HTO will be considered using only uranium as an example. The behavior of fission products during the nitriding process will be discussed in a separate publication.

2. Theoretical substantiation of the scheme of high-temperature processing of mixed nitride uranium-plutonium spent nuclear fuel (MNUP SNF)

In the U - N system, the existence of four nitrides has been established: UN, α-U_2N_3, β-U_2N_3 and UN_2 [9, 16]. Information on the existence of the $UN_{1.45}$, $UN_{1.55}$, $UN_{1.73}$, $UN_{1.75}$ (U_4N_7), $UN_{1.9}$ phases and a number of others [9, 17–19] is not always confirmed. The α-U_2N_3 and β-U_2N_3 phases are not polymorphic modifications since they have

Table 1 – Some properties of uranium oxides [9]. Here d – density; V_m – molar volume; ΔV_m – change in molar volume from UO_2.

Property	UO_2	α-U_3O_7	α-U_3O_8	α-UO_3
Melting point, °C	2865	Decomposes above 200 °C	1150 [a]	Decomposition after 450–500 °C
Crystal lattice	FCC (CaF_2 type)	Tetragonal	Orthorhombic, face-centered	Ortho-rhombic
Lattice period, nm	0.54704	a = 0.5447; c = 0.5400	a = 0.6716; b = 1.1960; c = 0.4147	a = 0.684; b = 4.345; c = 0.4157
d, g/cm^3	10.95	10.62	8.395	7.30
V_m, cm^3/mol	24.66	25.93	33.44	39.18
ΔV_m, %	–	+ 5.1	+ 36	+ 59
Weight gain, Δm	–	+ 1.98	+ 3.95	+ 5.93

[a] – In air it begins to decompose at 800–900 °C, but it decomposes completely only at 1300 °C ($U_3O_8 \rightarrow 3UO_2 + O_2$). In vacuum, the decomposition begins at 600 °C [10].

Table 2 – Composition of model fuel, compiled according to data [13–15].

Element	Content, mol. %	Element	Content, mol. %	Element	Content, mol. %
N	47.1	Zr	0.487	Pr	0.139
U	38.2	Nd	0.420	Sm	0.119
Pu	7.13	Pd	0.398	Am	0.117
C	1.49	Ce	0.275	H (T)	0.101
Xe	0.60	Ba	0.187	Sr	0.0912
Mo	0.569	Rh	0.156	Te	0.0862
Ru	0.525	La	0.148	Np	0.00013
Cs	0.501	Tc	0.143	Cm	$2.1 \cdot 10^{-7}$

different compositions [20–22]. The α-U_2N_3 phase is always excessive in nitrogen (α-U_2N_{3+x}). For this phase, the [N]/[U] ratio, according to various data, extends to 1.75–1.84. The β-U_2N_3 phase is nitrogen- deficient (β-U_2N_{3-y}) with a narrow homogeneity region. The [N]/[U] ratio is ~ 1.44–1.49. The β-U_2N_3 phase is obtained from the α-phase by removing nitrogen, via heating above 800–900 °C in a stream of inert gas or via vacuuming. The reverse $\beta \rightarrow \alpha$ transition in the absence of nitrogen (vacuum, inert atmosphere) does not occur even when the β-phase is cooled to the room temperature [23]. The β-$U_2N_3 \Rightarrow \alpha$-$U_2N_3$ transition occurs only when the chemical Reaction (6) occurs:

$$\beta\text{-}U_2N_{3-x} + xN_2 = \alpha\text{-}U_2N_{3+x}. \quad (6)$$

In Table 3, some properties of uranium nitrides are listed. We have not included the properties of the β-U_2N_3 phase in this table, since it does not play a significant role in the process described below, but we have added the $UN_{1.76}$ compound, which is sometimes interpreted as U_4N_7 [18, 24, 25]. The gross formula $UN_{1.76}$ corresponds formally to the 48 % $UN_{1.5}$ + 52 % UN_2 ratio, however, it has long been established that the $UN_{1.5}$ - UN_2 region is single phase [16, 26–28]. The $UN_{1.76}$ compound is of practical importance, since this is the maximum achievable [N]/[U] ratio at a nitrogen pressure of 1 atm [22, 28].

The entire $UN_{1.5}$ - UN_2 range is the region of a continuous solid solution. Nitride α-U_2N_3 has a wide homogeneity region and the $UN_{1.76}$ composition is still a superstoichiometric α-U_2N_3 phase with the initial BCC lattice of the Mn_2O_3 type [17, 20, 26, 32–34]. According to other data, the nitride α-U_2N_3 lattice is preserved up to the limiting ratio [N]/[U] = 1.75, and already at [N]/[U] = 1.76 and higher the FCC lattice of the dinitride UN_{2-x} is formed [27, 31, 36–38].

It has been noted that the oxygen impurity stabilizes the α-U_2N_3 phase and allows a higher [N]/[U] ratio to be achieved without transition to the UN_2 phase [22, 28, 31]. This apparently explains some of the differences in the results of different authors regarding the [N]/[U] ratio, at which the transition from the α-U_2N_3 phase to the UN_2 phase occurs. It is difficult to quantify the effect of oxygen since most articles do not provide its content in the initial nitrides. Some publications provide a detailed composition of impurities, but without specifying the oxygen content [28, 32, 39]. Limited data reported in [24, 35] indicate that, at an oxygen content of 0.2 wt. %, the α-U_2N_3 phase is preserved up to a ratio of [N]/[U] = 1.84. In our work, we will adhere to the limiting ratio for the α-U_2N_3 phase [N]/[U] = 1.76, since under industrial conditions, the UN or UN-PuN compounds always contain an oxygen impurity.

The crystalline lattice of α-U_2N_3 (FCC, Mn_2O_3 type) is actually a derivative of the FCC lattice of UN_2 (FCC type CaF_2), from which some nitrogen has been removed. The converse is also true, UN_2 is formed, when the α-U_2N_3 phase absorbs a sufficient amount of nitrogen. Therefore, the transition α-$U_2N_3 \rightarrow UN_2$ occurs smoothly, without a jump, and is detected only by structurally sensitive methods (X-ray, neutron diffraction) [34, 36, 39]. For example, Benz et al. [32] states that the α-U_2N_3, UN_2 phases and their solid solution were indistinguishable under a microscope. This transition is similar to the transitions $Ce_2O_3 \leftrightarrow CeO_2$, $Pr_2O_3 \leftrightarrow PrO_2$, $Tb_2O_3 \leftrightarrow TbO_2$, $Am_2O_3 \leftrightarrow AmO_2$, $Cm_2O_3 \leftrightarrow CmO_2$ [31, 37, 41].

Table 3 – Some properties of uranium nitrides according to [9].

Property	UN	α-U_2N_3 ($UN_{1.5}$)	$UN_{1.76}$ (U_4N_7)	UN_2 [22, 29, p. 318]
Melting point, °C	2850 [a]	~ 800 [b] [22] ~ 975 [c] [30]	–	675 [c] [30]
Crystal lattice	FCC, NaCl type	BCC, type Mn_2O_3	BCC, type Mn_2O_3 [24]	FCC type CaF_2
Lattice period, nm	0.4889	1.0678	1.0628	0.531
d, g/cm^3	14.32	11.24	≈ 11.4 [31]	11.73
V_m, cm^3/mol	17.60 17.59 [32]	23.05 22.9 [32]	≈ 23	22.68 22.0 [32]
ΔV_m, %	1	+ 30.9 % ≈ 30 % [33]	+ 30.9 %	+ 28.9 (–1.6 %)
Weight gain, Δm	1	+ 2.78 %	+ 4.22 %	+ 5.56 %

[a] – At a nitrogen pressure of about 2.5 atm;
[b] – Start of the decomposition in vacuum;
[c] – Beginning of the decomposition in an inert atmosphere. The decomposition is extended in temperature and time. Details are provided in [30].

Based on the properties of nitrides given in Table 3, we have proposed a scheme for the high-temperature treatment (HTT) of nitride SNF. The most complete scheme of the HTT of nitride SNF consists of the following operations: nitriding, denitriding, cladding separation, oxidation to U_3O_8 and reduction to UO_2. It is presented below as a sequence (7):

$$\begin{gathered} \mathrm{UN} \xrightarrow{\mathrm{N_2},\ 800\,^{\circ}\mathrm{C}} \mathrm{UN_{1.5}(UN_2)} \xrightarrow{\mathrm{Ar},\ 1200\,^{\circ}\mathrm{C}} \\ \mathrm{UN}\left[\begin{matrix}\text{Separation}\\ \text{of the cladding}\end{matrix}\right] \xrightarrow{\mathrm{Ar}+10\,\%\,\mathrm{O_2}} \\ \mathrm{U_3O_8} \xrightarrow{\mathrm{Ar},\ 1200\,^{\circ}\mathrm{C}} \mathrm{UO_2}. \end{gathered} \tag{7}$$

2.1. Nitriding

We will refer to nitriding as the process, in which the initial UN or nitride SNF is kept in a nitrogen flow at 800–850 °C. In this case, Reactions (8), (9) occur sequentially:

$$\mathrm{UN} + 0.25\mathrm{N_2} = \mathrm{UN_{1.5}}, \tag{8}$$

$$\mathrm{UN_{1.5}} + 0.13\mathrm{N_2} = \mathrm{UN_{1.76}}. \tag{9}$$

The change in Gibbs energy during Reactions (8) and (9) is shown in Figure 1. All thermodynamic calculations were performed using the HSC Chemistry 9.9 software package and its built-in database of thermodynamic properties of substances [42].

According to the data given in Table 2, during Reactions (8) and (9), uranium mononitride, which has the FCC lattice, is transformed into α-U_2N_3 with the BCC lattice with a lower atomic packing density (two atoms per unit BCC cell versus four for the FCC cell). The fuel volume increases by approximately 30 %, which will cause expanding or rapture of the fuel element cladding. The transformation of nitride with one crystal lattice into nitride with another lattice facilitates the dispersion of the fuel and the release of volatile fission products. As can be seen in Figure 1, with increasing temperature, the change in the Gibbs energy (ΔG) of the nitriding reactions shifts to the positive side. However, ΔG of the reactions remains negative, and an increase in the temperature, for example from 800 to 850 °C, will accelerate the reaction.

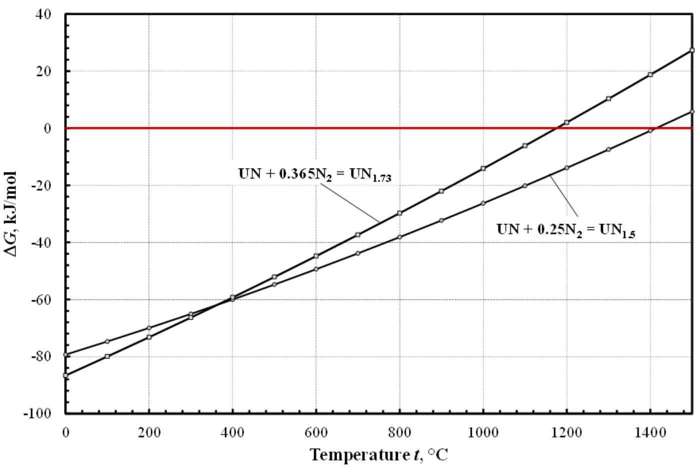

Figure 1 Total change in the Gibbs energy during Reactions (8) and (9) at the $p(N_2)$ = 1 atm. The HSC program database does not contain any thermodynamic data on nitride $UN_{1.76}$, so the calculation was made for the almost identical $UN_{1.73}$.

2.2. Denitriding

The denitriding operation is the decomposition of uranium nitrides $UN_{1.76} \rightarrow UN$, obtained in the previous operation, in a vacuum or inert atmosphere at elevated temperature. In this case, the fuel volume decreases by 30 % (Table 2), and the fuel element cladding remains expanded. In addition, the BCC phase of $UN_{1.76}$ with the BCC lattice is replaced by the FCC phase of UN. This transformation also leads to grinding of the fuel and promotes the release of volatile fission products.

When $UN_{1.76}$, obtained at the nitriding stage, is heated in a flow of argon at 1100–1200 °C, decomposition reactions occur. These Reactions (10) and (11) are the reverse Reactions of (8) and (9):

$$\begin{gathered}\mathrm{UN_{1.73}} = \mathrm{UN_{1.5}} + 0.115\mathrm{N_2}, \\ \Delta G = -18.7\ \mathrm{kJ/mol\ at\ 1200\ ^{\circ}C}\end{gathered} \tag{10}$$

$$\begin{gathered}\mathrm{UN_{1.5}} = \mathrm{UN} + 0.25\mathrm{N_2}, \\ \Delta G = +16.7\ \mathrm{kJ/mol\ at\ 1200\ ^{\circ}C}\end{gathered} \tag{11}$$

As can be seen, at such a temperature intermediate nitride $UN_{1.73}$ ($UN_{1.76}$) decomposes only to $UN_{1.5}$. Further decomposition of this nitride at such a temperature does not occur spontaneously. The change in Gibbs energy during Reaction (12) is positive. However, the reaction product is nitrogen, and if it is removed from the reaction zone, the equilibrium will constantly shift towards the products. This statement can be characterized quantitatively. For example, at nitrogen pressure of 0.0001 atm (~ 10 Pa) the Gibbs free energy change for Reaction (11) will change by –11 kJ making this reaction clearly possible.

Figure 2 shows the nitrogen vapor pressure in the UN-$UN_{1.76}$ system depending on the temperature according to data from [39, 43]. These are the most different data reported in the literature; however, it is clear that they are practically identical.

Other data are collected in [36]. At 1100 °C the nitrogen pressure is 34 mm Hg, and at 1200 °C it is already 133 mm Hg. This is sufficient for nitrogen to be

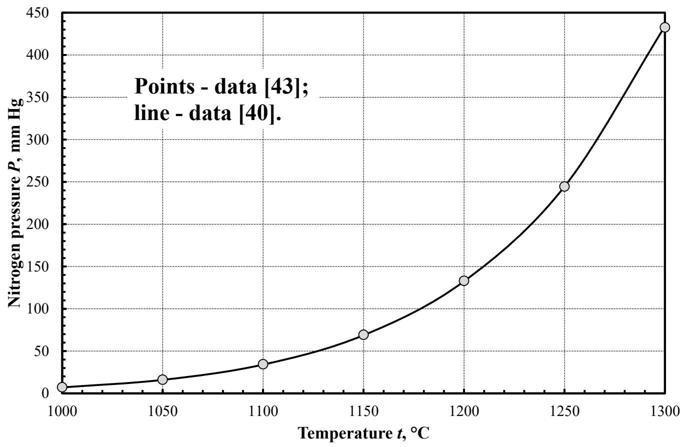

Figure 2 Nitrogen vapor pressure in the UN-$UN_{1.76}$ system depending on temperature.

gradually removed in a stream of argon. However, this is still a much slower reaction than nitriding.

The decomposition of $UN_{1.76}$ at the temperatures above 800 °C in an inert atmosphere should theoretically lead to the formation of a nitrogen-deficient phase β-U_2N_3, which will further decompose to UN. However, in [30, 36] it was noted that β-U_2N_3 was not detected during the decomposition of higher nitrides. This may be due to the presence of oxygen in the samples, which stabilizes the α-phase. For example, in the work [30] it is indicated that UN-U_2N_3 samples contained 2.2–3.2 % UO_2.

At the stages of nitriding and denitriding, volatile fission products can be removed: inert gases, cesium, rubidium, cadmium.

2.3. Separation of the cladding

During nitriding and denitriding operations, the cladding material does not enter into any chemical interactions and does not contaminate the fuel [44]. Therefore, the cladding should be separated from the fuel after denitriding, before the start of oxidation, using sieving, magnetic separation, or other methods.

2.4. Voloxidation and reduction

The ultimate goal of the HTT is to obtain uranium dioxide, which is well pressed into tablets suitable for subsequent electrochemical reduction (metallization) [1–3]. Both metallic uranium and its compounds usually yield triuranium octoxide, U_3O_8, when oxidized. Therefore, UO_2 is obtained sequentially in two stages - oxidation and then partial reduction.

2.4.1. Voloxidation (oxidation)

There are dozens of published works devoted to the oxidation of uranium mononitride with oxygen, air, nitrogen oxides, carbon monoxide, water vapor, nitric acid and all kinds of their mixtures with argon and with each other. Kul'ykhin et al. [45] reviewed the majority of works devoted to the UN oxidation. The voloxidation process is described in detail in work reported by several authors [46–50].

The probable oxidation reactions of UN are as follows:

$$\mathrm{UN + O_2 = UO_2 + 0.5N_2}, \quad (12)$$

$$\mathrm{UN + 1.167O_2 = 0.333U_3O_7 + 0.5N_2}, \quad (13)$$

$$\mathrm{UN + 1.333O_2 = 0.333U_3O_8 + 0.5N_2}, \quad (14)$$

$$\mathrm{UN + 1.5O_2 = UO_3 + 0.5N_2}. \quad (15)$$

The change in Gibbs energy during Reactions (12)–(15) is illustrated in Figure 3. As can be seen from this figure, ΔG of these reactions are close to each other and, therefore, all these reactions occur simultaneously, although in different proportions.

Oxides have different thermal stability. Figure 3 illustrates the solid lines break off at the point, where thermal decomposition begins. However, in solid solutions, the thermal stability of substances can be significantly higher.

In addition to Reactions (12)–(15), oxidation reactions with the formation of nitrogen oxides are thermodynamically possible:

$$\mathrm{UN + 1.583O_2 = 0.333U_3O_8 + 0.5N_2O}, \quad (16)$$

$$\mathrm{UN + 1.833O_2 = 0.333U_3O_8 + NO}, \quad (17)$$

$$\mathrm{UN + 2.333O_2 = 0.333U_3O_8 + 0.5NO_2}, \quad (18)$$

$$\mathrm{UN + 2.583O_2 = 0.333U_3O_8 + 0.5N_2O_5}. \quad (19)$$

The change in Gibbs energy during Reactions (16)–(19) is shown in Figure 4.

According to [51], N_2O decomposes into elements above 500 °C, NO is thermally stable up to 1000 °C, but in the presence of oxygen it is immediately oxidized to NO_2, N_2O_3 is stable below –4 °C; N_2O_5 gradually decomposes above +10 °C. Thus, only nitrogen dioxide, NO_2, should be taken into account.

The thermodynamic modeling of the equilibrium composition formed during the UN treatment with a gas mixture of (Ar + 20 % O_2) at 850 °C was performed. The results are shown in Figure 5.

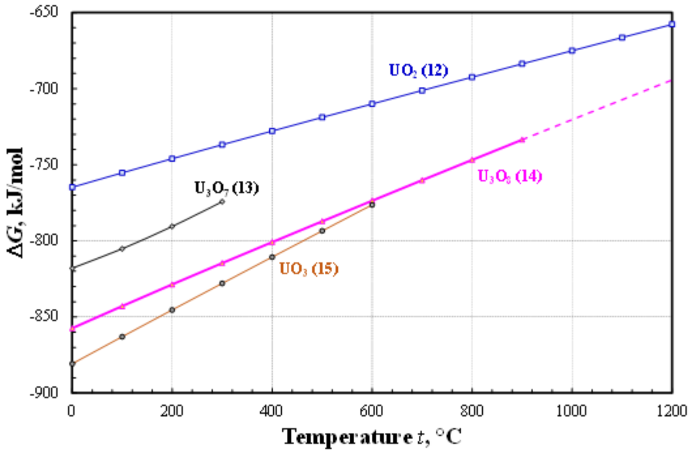

Figure 3 Change in Gibbs energy during Reactions (12)–(15) depending on temperature.

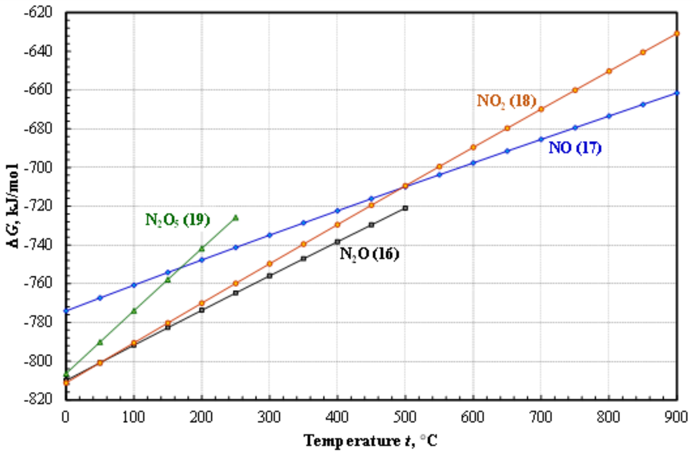

Figure 4 Change in Gibbs energy during Reactions (16)–(19) depending on temperature.

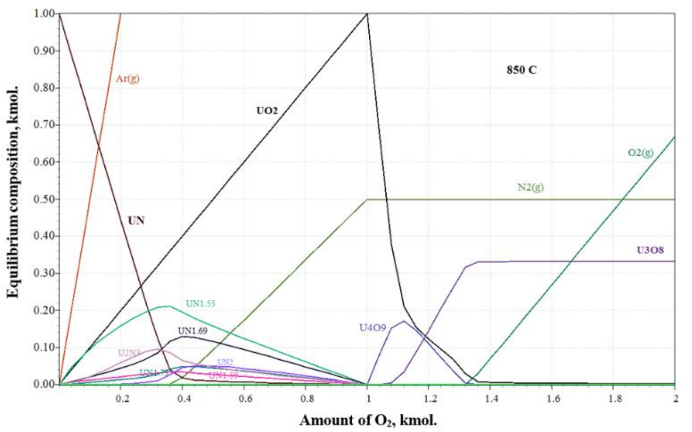

Figure 5 Equilibrium composition formed during the treatment of UN with a gas mixture (Ar + 20 % O_2) at 850 °C.

The simulation results indicate that the process proceeds in a complex manner through a number of intermediate products. During the initial oxidation stage (up to ~ 0.36 kmol of O_2 flow), released nitrogen does not flow to the gas phase, it interacts with unoxidized UN with the formation of a mixture of higher nitrides ($UN_{1.51}$, $UN_{1.55}$, $UN_{1.59}$, $UN_{1.69}$, $UN_{1.73}$). This mixture of nitrides is the same as nitrogen-superstoichiometric α-$UN_{1.5+x}$. That is, uranium is oxidized both by oxygen and by released nitrogen.

When the amount of O_2 flow exceeds ~ 0.36 kmol, nitrogen evolves into the gas phase and a fracture of higher nitrides decreases. This is confirmed by the experimental data [45, 52, 53].

At a ratio of UN : O_2 = 1 : 1 (mol.) individual UO_2 is formed. Upon further treatment with a gas mixture (Ar + O_2), a mixture (UO_2 + U_4O_9 + U_3O_8) is formed, which is converted into individual U_3O_8, when approximately 1.4 mol of O_2 per 1 mol of the initial UN is passed. The sequence of transformations is shown in the Scheme (20):

$$\mathrm{UN} \rightarrow (\alpha\text{-}\mathrm{UN}_{1.5+x} + \mathrm{UO_2}) \rightarrow \mathrm{UO_2} \rightarrow \\ \rightarrow (\mathrm{UO_2} + \mathrm{U_4O_9} + \mathrm{U_3O_8}) \rightarrow \mathrm{U_3O_8}. \qquad (20)$$

The high process temperature (800–850 °C) was chosen to exclude the formation of UO_3, see Table 1.

Theoretically, when passing a stoichiometric amount of oxygen (UN : O_2 = 1 : 1 mol), it is possible to obtain UO_2 already at the oxidation stage, if the oxidizer at the right moment is not supplied. In practice, this is unlikely to be feasible since, in a real apparatus, the reaction may proceed unevenly. In addition, an excess of oxidizer is usually used to complete the reaction. Therefore, UN is oxidized to U_3O_8 and then the operation of reducing U_3O_8 to UO_2 is necessary.

The equilibrium composition shown in Figure 5 does not contain nitrogen oxides. However, it should be noted that this is the equilibrium composition in a closed system. According to the data illustrated in Figure 4, the formation of nitrogen oxides is very likely from the thermodynamic point of view. But in the closed system they are totally consumed for the UN oxidation. For instance, nitrogen dioxide itself is a strong oxidizer and a number of studies have proposed using it to oxidize SNF [47, 48]:

$$\mathrm{UN} + 1.333\mathrm{NO_2} = 0.333\mathrm{U_3O_8} + 1.167\mathrm{N_2}, \\ \Delta G = -881 \text{ kJ at } 850\ °\mathrm{C} \qquad (21)$$

2.4.2. Reduction

The thermal reduction of U_3O_8 to UO_2 occurs according to Reaction (22).

$$U_3O_8 = 3UO_2 + 3O_2. \quad (22)$$

The change in Gibbs energy during Reaction (22) is shown in Figure 6. It is positive over the entire temperature range. Therefore, the reaction can proceed only due to a shift in equilibrium associated with the removal of oxygen from the reaction zone, similar to Reaction (11).

The oxygen pressure over U_3O_8 as a function of temperature is shown in Figure 7. According to [54], at 1200 °C this pressure is only ~ 65 Pa. Therefore, such reduction can be expected to proceed slowly.

The reaction can be significantly accelerated, and the temperature can be lowered if an argon-hydrogen mixture is used instead of argon. In this case, the reduction occurs according to Reaction (23):

$$U_3O_8 + H_2 = UO_2 + H_2O, \quad \Delta G = -69 \text{ kJ at } 600 \text{ °C} \quad (23)$$

The recommended temperature is 400–650 °C. Above 650 °C, the rate of this reaction does not increase due to some sintering of the UO_2 powder [55, 56].

There are other methods of reduction described in the literature. Thus, in article [57] it is stated that if U_3O_8 oxide is immersed into the LiCl-Li_2O melt, then U_3O_8 is spontaneously reduced to UO_2.

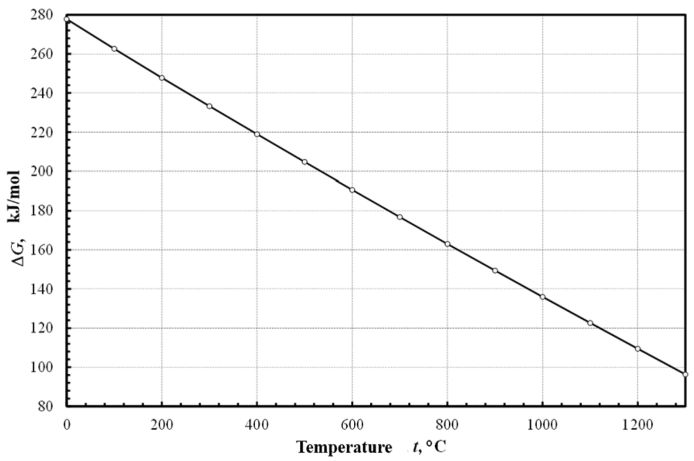

Figure 6 Change in Gibbs energy during Reaction (22) depending on temperature.

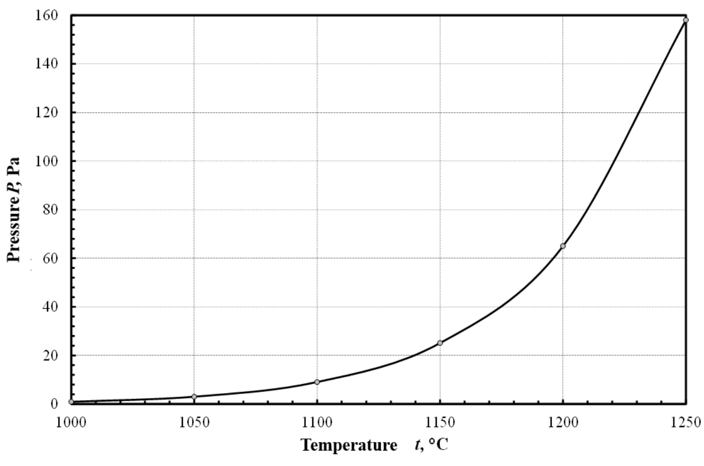

Figure 7 Oxygen pressure over U_3O_8 according to [54].

3. Conclusions

1. The properties of uranium oxides and nitrides were analyzed and compared.

2. Based on the difference in the properties of lower and higher nitrides and oxides of uranium, a method for high-temperature reprocessing of nitride spent nuclear fuel has been proposed and substantiated.

3. The proposed method consists of successive operations: nitriding – denitriding – cladding separation – oxidation – reduction. Uranium dioxide UO_2 is a target product that is suitable for pressing and transfer to the reduction stage.

4. The next step should be an experimental verification of the proposed method for reprocessing nitride spent nuclear fuel.

Supplementary materials

No supplementary materials are available.

Funding

This research was performed within the frame of the budget plan of the Institute of High Temperature Electrochemistry of the Ural Branch of the Russian Academy of Sciences.

Acknowledgments

None.

Author contributions

Alexey M. Potapov: Conceptualization; Data curation; Formal Analysis; Investigation; Writing – Original draft, Writing – Review & Editing.

Mikhail V. Mazannikov: Resources; Software; Validation; Visualization.

Yury P. Zaikov: Funding acquisition; Methodology; Project administration; Supervision.

Conflict of interest

The authors declare no conflict of interest.

Additional information

Alexei Potapov, Scopus Author ID: 56962735400; ORCID ID: 0000-0001-7372-581X;

Mikhail Mazannikov, Scopus Author ID: 57218353097; ORCID ID: 0000-0003-1160-7177;

Yuriy Zaikov, Scopus Author ID: 6603601069; ORCID ID: 0000-0001-6138-3955.

References

1. Shishkin AV, Shishkin VY, Salyulev AB, Kesikopulos VA, et al., Electrochemical reduction of uranium dioxide in LiCl–Li$_2$O melt, At. Energy, **131(2)** (2021) 77–82. https://dx.doi.org/10.1007/s10512-022-00850-y

2. Shishkin AV, Shishkin VY, Pankratov AA, Burdina AA, Zaikov YP, Electrochemical reduction of La$_2$O$_3$, Nd$_2$O$_3$, and CeO$_2$ in LiCl-Li$_2$O melt, Materials, **15(11)** (2022) 3963. https://dx.doi.org/10.3390/ma15113963

3. Shishkin AV, Shishkin VY, Maslennikova AA, Salyulev AB, et al., Electrochemical reduction of Pd-Nd$_2$O$_3$-CeO$_2$ mixtures in the LiCl-Li$_2$O melt, Processes, **11(6)** (2023) 1599. https://dx.doi.org/10.3390/pr11061599

4. Zaikov YP, Shishkin VY, Potapov AM, Dedyukhin AE, et al., Research and development of the pyrochemical processing for the mixed nitride uranium-plutonium fuel, J. Phys. Conf. Ser., **1475(1)** (2020) 012027. https://dx.doi.org/10.1088/1742-6596/1475/1/012027

5. Goode JH. Voloxidation – removal of volatile fission products from spent LMFBR fuel (ORNL-TM-3723). Oak Ridge National Laboratory; 1973. 133 p. https://www.osti.gov/biblio/4587712

6. Stone JA. Voloxidation studies with UO$_2$ reactor fuels. American Nuclear Society topical meeting on "Fuel Cycles for the Eighties" DP-MS-80-9; 1980. 15 p.

7. Song KW, Yang MS, Formation of columnar U$_3$O$_8$ grains on the oxidation of UO$_2$ pellets in air at 900 °C, J. Nucl. Mater., **209(3)** (1994) 270–273. https://dx.doi.org/10.1016/0022-3115(94)90262-3

8. Yoo JH, Seo C-D, Kim EH, et al., A conceptual study of pyroprocessing for recovering actinides from spent oxide fuels, Nucl. Eng. Technol., **40(7)** (2008) 581–592. https://dx.doi.org/10.5516/net.2008.40.7.581

9. Grenthe I, Janusz Drożdżyński J, Fujino T, et al. Uranium. In: The chemistry of the actinide and transactinide elements. 3rd ed. Springer: Dordrecht; 2008. 253–698 p. https://doi.org/10.1007/1-4020-3598-5_5

10. Thein SM, Bereolos PJ, Thermal Stabilization of ^{233}UO$_2$, ^{233}UO$_3$, and ^{233}U$_3$O$_8$. Oak Ridge National Laboratory: ORNL/TM-2000/82; 2000. 15 p.

11. Kulyukhin SA, Nevolin YM, Gordeev AV, Gas-phase conversion of uranium mononitride in a nitrating atmosphere, Radiochemistry, **61(1)** (2019) 5–11. https://dx.doi.org/10.1134/s1066362219010028

12. Johnson J, Rawn C, Spencer B, Meisner R, Del Cul G, Oxidation kinetics for conversion of U$_3$O$_8$ to ε-UO$_3$ with NO$_2$, J. Nucl. Mater., **490** (2017) 211–215. https://dx.doi.org/10.1016/j.jnucmat.2017.03.048

13. Arai Y, Maeda A, Shiozawa K, Ohmichi T, Chemical forms of solid fission products in the irradiated uranium–plutonium mixed nitride fuel, J. Nucl. Mater., **210(1–2)** (1994) 161–166. https://dx.doi.org/10.1016/0022-3115(94)90233-x

14. Lyubimov DY, Androsov AV, Bulatov GS, Gedgovd KN, Thermodynamic modeling of the phase composition of mixed uranium-plutonium mononitride under fast-neutron irradiation to burnup 80 GW·days/ton and temperature 900–1400 K, At. Energy, **114(4)** (2013) 243–248. https://dx.doi.org/10.1007/s10512-013-9704-0

15. Bondarenko GG, Bulatov GS, Gedgovd KN, Lyubimov DY, Yakushkin MM, Effect of the electron decay of metallic fission products on the chemical and phase compositions of an uranium-plutonium fuel irradiated by fast neutrons, Russ. Met. (metally), **2011(11)** (2011) 1074–1078. https://dx.doi.org/10.1134/s0036029511110036

16. Alekseev SV, Zaitsev VA. Nitridnoye toplivo dly yadernoy energii [Nitride fuel for nuclear power]. Moscow: Technosfera; 2013. 240 p. Russian.

17. Berthold HJ, Delliehausen C, Darstellung und röntgenographische Untersuchung höherer Urannitride, Angew. Chemie, **78(15)** (1966) 750–751. https://dx.doi.org/10.1002/ange.19660781512

18. Kim WJ, Nam JM, Ryu HJ, et al. Analyses of interaction phases of U-Mo dispersion fuel by synchrotron X-ray diffraction. In: Transactions of the Korean Nuclear Society Autumn Meeting; 2012 Oct 25–26; Gyeongju, Korea. p. 12.

19. Yungman VS, Glushko VP, Medvedev VA, Gurvich LV. Thermal constants of substances. Vol. 1–8. New York: Consultants Bureau; 1999. 1200 p.

20. Sasa Y, Atoda T, Nonstoichiometric hexagonal close-packed uranium sesquinitride, J. Am. Ceram. Soc., **53(2)** (1970) 102–105. https://dx.doi.org/10.1111/j.1151-2916.1970.tb12020.x

21. Uno M, Nishi T, Takano M. Thermodynamic and thermophysical properties of the actinide nitrides. In: Comprehensive Nuclear Materials. Vol. 2. Elsevier Ltd: Amsterdam; 2012. 61–85 p. https://doi.org/10.1016/B978-0-08-097774-4.00202-1

22. Kotelnikov RB, Bashlykov SN, Kashtanov AI, Menshikova TS. Vysokotemperaturnoye yadernoye toplivo [High temperature nuclear fuel]. Moscow: Atomizdat; 1978. 432 p. Russian.

23. Stöcker HJ, Naoumidis A, Investigation of the kinetics of hydrogen peroxide decomposition on manganese dioxide, Berichte der Deutschen Botanischen Gesellschaft, **79(12)** (1966) 1231–1238. https://doi.org/10.1111/j.1438-8677.1966.tb00557.x

24. Serizawa H, Fukuda K, Ishii Y, Funahashi S. Diffraction study on the nonstoichiometric α-U$_2$N$_{3+x}$ phase. In: Proceedings of the Fifth International Symposium on Advanced Nuclear Energy Research "Neutrons as Microscopic Probes"; 1993 Mar 10–12; Mito, Japan. p. 45.

25. Pavliuk AO, Zagumennov VS, Kotlyarevskiy SG, Bespala EV, Thermodynamic simulation of equilibrium composition of reaction products at dehydration of a technological channel in a uranium-graphite reactor, Therm.

Eng., **65(1)** (2018) 51–56. https://dx.doi.org/10.1134/s0040601518010056

26. Matthews R, Chidester K, Hoth C, Mason R, Petty R, Fabrication and testing of uranium nitride fuel for space power reactors, J. Nucl. Mater., **151(3)** (1988) 345. https://dx.doi.org/10.1016/0022-3115(88)90029-3

27. Rundle RE, Baenziger NC, Wilson AS, Mcdonald RA, The structures of the carbides, nitrides and oxides of uranium, J. Am. Chem. Soc., **70(1)** (1948) 99–105. https://dx.doi.org/10.1021/ja01181a029

28. Benz R, Balog G, Baca BH, U-UO_2-UN_2 phase diagram, High temperature Sci., **2(2)** (1970) 221–251. https://dx.doi.org/10.1021/ic0500199.s002

29. Novyi spravochnik khimika i tekhnologa. Osnovnye svoistva neorganicheskikh, organicheskihk y elemetoorganicheskikh soedineniy [New reference book for chemists and technicians. Main properties of inorganic, organic and elementorganic compounds]. Saint Petersburg: NPO "Mir i Sem'ya"; 2002. 1276 p. Russian.

30. Silva GW, Yeamans CB, Sattelberger AP, Hartmann T, et al., Reaction sequence and kinetics of uranium nitride decomposition, Inorg. Chem., **48(22)** (2009) 10635–10642. https://dx.doi.org/10.1021/ic901165j

31. Tagawa H, Masaki N, X-ray and density studies of nonstoichiometric uranium sesquinitride, J. Inorg. Nucl. Chem., **36(5)** (1974) 1099–1103. https://dx.doi.org/10.1016/0022-1902(74)80220-4

32. Benz R, Hutchinson WB, U + N_2 Reaction layer growths, J. Nucl. Mater., **36(2)** (1970) 135–146. https://dx.doi.org/10.1016/0022-3115(70)90137-6

33. Hoenig CL, Phase equilibria, vapor pressure, and kinetic studies in the uranium-nitrogen system, J. Am. Ceram. Soc., **54(8)** (1971) 391–398. https://dx.doi.org/10.1111/j.1151-2916.1971.tb12329.x

34. Trzebiatowski W, Troć R, Magnetic properties of uranium nitrides. The U_2N_3 phase of variable composition, Bulletin de l'académee Polonaise des sciences, Serie des sciences chimiques, **12** (1964) 10681–685. https://dx.doi.org/10.2307/2270953

35. Serizawa H, Fukuda K, Ishii Y, Morii Y, Katsura M, Crystallographic study on the phase transition of α-U_2N_3, J. Nucl. Mater., **208(1–2)** (1994) 128–134. https://dx.doi.org/10.1016/0022-3115(94)90204-6

36. Hiroaki T, Phase relations and thermodynamic properties of the uranium-nitrogen system, J. Nucl. Mater., **51(1)** (1974) 78–89. https://dx.doi.org/10.1016/0022-3115(74)90117-2

37. Masaki N, Tagawa H, Diffraction study of α-U_2N_{3+x}, J. Nucl. Mater., **57(2)** (1975) 187–192. https://dx.doi.org/10.1016/0022-3115(75)90258-5

38. Evans P, Davies T, Uranium nitrides, J. Nucl. Mater., **10(1)** (1963) 43–55. https://dx.doi.org/10.1016/0022-3115(63)90115-6

39. Katsura M, Serizawa H, Formation of a nitrogen-rich α-U_2N_{3+x} phase by the reaction of uranium with a stream of ammonia, J. Alloy. Compd., **187(2)** (1992) 389–399. https://dx.doi.org/10.1016/0925-8388(92)90444-e

40. Bugl J, Bauer AA, Phase relations in the system uranium–nitrogen, J. Am. Ceram. Soc., **47(9)** (1964) 425–429. https://dx.doi.org/10.1111/j.1151-2916.1964.tb14429.x

41. Tagawa H, Equilibrium nitrogen pressures and thermodynamic properties of uranium sesquinitride, J. Nucl. Mater., **41(3)** (1971) 313–319. https://dx.doi.org/10.1016/0022-3115(71)90168-1

42. Roine A. HSC Chemistry® [Software]. Outotec: Pori; 2018. Available from: www.outotec.com/HSC, Accessed on 19.11.2025.

43. Katsura M, Sano T, The uranium-nitrogen system, J. Nucl. Sci. Technol., **4(6)** (1967) 283–288. https://dx.doi.org/10.3327/jnst.4.283

44. Karfidov EA, Nikitina EB, Mazannikov MV, Potapov AM, Dedyukhin AE, Corrosion of EP-823 steel (16Kh12MVSFBR) under high-temperature spent nuclear fuel processing, Rasplavy (Melts), **6** (2024) 581–595. Russian. https://dx.doi.org/10.31857/S0235010624060014

45. Kulyukhin SA, Nevolin YM, Gordeev AV, Bessonov AA, Gas-phase volume oxidation of uranium mononitride, Radiochemistry, **61(2)** (2019) 146–155. https://dx.doi.org/10.1134/s1066362219020036

46. Mazannikov MV, Potapov AM, Vylkov AI, Suzdaltsev AV, Zaykov YuP, inventors; Institute of High-Temperature Electrochemistry UB RAS, assignee. Sposob okislitelnoy obrabotki otrabotavshego nitridnogo yadernogo topliva. Russian Federation patent RU 2775563. 2021 Dec 21. Russian.

47. McEachern RJ, Sunder S, Taylor P., Doern DC, et al., The influence of nitrogen dioxide on the oxidation of UO_2 in air at temperatures below 275 °C, J. Nucl. Mat., **255** (1998) 234–242. https://doi.org/10.1016/S0022-3115(98)00036-1

48. Nevolin YuM. Gas phase oxidation conversion of components of oxide, nitride and carbide spent nuclear fuel [dissertation]. Moscow (Russia); 2020. 18 p.

49. Momotov VN, Makarov AO, Volkov AY, Lakeev PV, et al., Voloxidation of mixed nitride uranium–plutonium spent nuclear fuel, Radiochemistry, **65(2)** (2023) 177–184. https://dx.doi.org/10.1134/s1066362223020042

50. Shadrin A, Dvoeglazov K, Kascheyev V, Vidanov V, et al., Hydrometallurgical reprocessing of BREST-OD-300 mixed uranium-plutonium nuclear fuel, Procedia Chem., **21** (2016) 148–155. https://dx.doi.org/10.1016/j.proche.2016.10.021

51. Knunyants IL. Chemical encyclopedia. In 5 volumes. Moscow: Soviet encyclopedia; 1988, 625 p. Russian.

52. Dell RM, Wheeler VJ, Mciver EJ, Oxidation of uranium mononitride and uranium monocarbide, Trans. Faraday Soc., **62** (1966) 3591. https://dx.doi.org/10.1039/tf9666203591

53. Sole MJ, Van der Walt CM, Oxidation and deformation studies of uranium nitride by electron microscopy, Acta Met., **16(4)** (1968) 501–510. https://dx.doi.org/10.1016/0001-6160(68)90124-7

54. Blackburn PE, Oxygen dissociation pressures over uranium oxides, J. Phys. Chem., **62(8)** (1958) 897–902. https://dx.doi.org/10.1021/j150566a001

55. Volkovich VA, Smirnov AL. Uranium metallurgy and technology of its compounds. Part 3. Ekaterinburg; 2014. 140 p.

56. Gromov BV. Introduction to chemical engineering of uranium. Moscow: Atomizdat; 1978. 336 p.

57. Hur J, Choi I, Cho S, Jeong S, Seo C, Preparation and melting of uranium from U_3O_8, J. Alloy. Compd., **452(1)** (2008) 23–26. https://dx.doi.org/10.1016/j.jallcom.2006.11.210